Pushing EUV lithography development beyond 22-nm half pitch

Patrick P. Naulleau,[1] Christopher N. Anderson,[2] Lorie-Mae Baclea-an,[1] Paul Denham,[1] Simi George,[1] Kenneth A. Goldberg,[1] Michael Goldstein,[3] Brian Hoef,[1] Gideon Jones,[1] Chawon Koh,[3] Bruno La Fontaine,[4] Warren Montgomery,[3] and Tom Wallow[4]

[1] Center for X-Ray Optics, Lawrence Berkeley National Laboratory, Berkeley, CA 94720
[2] Applied Sci. & Technol. Graduate Group, University of California, Berkeley, CA 94720
[3] SEMATECH, Albany, NY 12203
[4] Advanced Micro Devices, Sunnyvale, CA 94088

Abstract

Microfield exposure tools (METs) have and continue to play a dominant role in the development of extreme ultraviolet (EUV) resists and masks. One of these tools is the SEMATECH Berkeley 0.3 numerical aperture (NA) MET. Here we investigate the possibilities and limitations of using the 0.3-NA MET for sub-22-nm half-pitch development. We consider mask resolution limitations and present a method unique to the centrally obscured MET allowing these mask limitations to be overcome. We also explore projection optics resolution limits and describe various illumination schemes allowing resolution enhancement. At 0.3-NA, the 0.5 k_1 factor resolution limit is 22.5 nm meaning that conventional illumination is of limited utility for sub-22-nm development. In general resolution enhancing illumination encompasses increased coherence. We study the effect of this increased coherence on line-edge roughness, which along with resolution is another crucial factor in sub-22-nm resist development.

1. Introduction

Despite the recent availability of full field extreme ultraviolet (EUV) alpha tools [1, 2], microfield exposure systems [3-5] continue to play a crucial role in the development of EUV lithography. This is especially true now that advanced development has started to focus on sub-22 half-pitch resolution. Figure 1 shows Prolith [6] modeling results of the

limits of a tool with a numerical aperture (NA) of 0.25 and conventional disk illumination with coherence factor of 0.5. Moreover, we have assumed 7% effective flare and 1 nm of aberrations randomly distributed over Zernikes 5 through 37. We note that Zernikes 1 through 4 are piston, x tilt, y tilt, and defocus, respectively. Taking the resolution limit to correspond to a contrast of 50%, the modeling results predict a resolution limit of 27 nm half pitch which correlates well with published experimental results [7]. Evidently, sub-22-nm half pitch development is not feasible with such tools.

Considering instead 0.3-NA microfield tools, modeling results show similar limitations when utilizing conventional illumination. Figure 2 shows the aerial-image contrast as a function of half pitch for the SEMATECH Berkeley microfield exposure tool (BMET) with annular illumination illumination ($0.35 < \sigma < 0.55$). Flare and wavefront aberration values are taken from the literature [8,9]. Here we find the 50% contrast resolution limit to be 22 nm. Even at 0.3 NA it is not possible to enter the sub-22-nm regime using conventional illumination and masks. A significant benefit of the BMET, however, is that it enables lossless variable illumination allowing resolution enhancement to be implemented. Figure 3 shows the aerial-image modeling results for four different resolution enhancing illumination settings. In all cases vertical lines and spaces are modeled, but we note that the two 45°-rotated dipoles are capable of imaging Manhattan geometry (both horizontal and vertical lines). For the x-oriented dipole cases, only vertical lines resolution is enhanced and the system suffers from forbidden pitches due to the central obscuration in the projection optics. Based on the 50% aerial-image contrast criterion, all cases support sub-22-nm half pitch resolution with the most aggressive case supporting 12-nm half pitch.

2. Demonstration of resolution enhancing illumination

It is evident that the ability to control illumination conditions is crucial to the attainment of sub-22-nm resolution in current EUV tools. Figure 4 demonstrates that illumination control in the BMET is indeed possible and the results predictable. Shown is the direct comparison of printing and modeling results for radial gratings of varying half pitch using 45°-rotated dipole illumination with a pole radius of 0.15 and offset of 0.57. The orientation and pitch dependence of the imaging performance is clear and correlates well between modeling and experiment. Having confidence in the illumination control, we further use the 45°-rotated dipole to print vertical lines and spaces as shown in Fig. 5. Good printing performance is seen down to 20 nm. Next we consider x-oriented dipole illumination (Fig. 6). Despite the significantly improved expected aerial image, we again see a resolution limit in resist of approximately 20 nm.

The above results raise the question about the mask: could the mask also be contributing to the observed resolution limit? Figure 7 shows scanning electron micrographs from the EUV reticle used on the BMET demonstrating that the mask itself also suffers from a limit of approximately 20 nm. We note that similar results have been found on masks from other suppliers.

2. Getting around mask resolution limits

Mask resolution limitations can be significantly mitigated through a process we refer to as pseudo strong phase shift mask. In strong phase shift mask technology, the zeroth diffraction order from the object is suppressed by virtue of destructive interference which in turns leads to the printed pitch being one half the patterned pitch on the mask (in addition to the normal system demagnification). Strong phase shift mask technology,

however, is not readily available at EUV due to the complex mask fabrication process. However, with a centrally obscured optic, the same effect of zeroth order suppression can readily be achieved by ensuring the pupil fill is completely blocked by the obscuration (Fig. 8). The zeroth order transmitted by the conventional binary amplitude mask being restricted in the pupil to the actual area of the illumination pupil fill will be blocked. This leads to an image plane electric field that is essentially indistinguishable from that would have appeared had a strong phase shift mask been used. The ultimate resolution limit of this method is identical to the extreme dipole case, or approximately 12-nm half pitch for the BMET design, however, the mask pitch is relaxed by a factor of two.

Figure 9 shows printing results in the pseudo strong phase shift mask mode. On-axis disk illumination with a coherence factor of 0.15 was used. Note that the BMET central obscuration is 30% of the full pupil in radius. The printing results again show a resolution limit of approximately 20 nm suggesting that the resist is indeed the limiting factor.

3. Mask roughness limitations

For both the resolution enhanced illumination and pseudo strong phase shift mask cases, low sigma high coherence illumination is required. It has been shown, however, such illumination conditions render the process significantly more susceptible to multilayer-roughness induced phase variations on the mask [10-13]. Thus modeling is used to study the potential importance of these effects to the pseudo strong phase shift mask results presented here. For details on the modeling procedure and the mask metrology performed to determine the required mask characteristics, the reader is referred to Ref. [12]. Figure 10 shows aerial-image results as well as thresholded versions showing the strong impact

of mask effects on the LER. Again we find that the mask in addition to the resist is leading to printing limitations in the sub-22-nm regime.

4. Summary

Achieving sub-22-nm half pitch resolution with current 0.25 and 0.3-NA EUV tools requires the use of modified illumination or other resolution enhancement methods. The BMET has been used to demonstrate sub-22-nm printing with both modified illumination and a spatial filtering method akin to strong phase shift mask technology yet compatible with conventional binary amplitude masks. These techniques, however, all rely on high spatial coherence which appears to give rise to unacceptably large mask-induced LER effects. Ultimately, to address development at the 16-nm half pitch node, higher-NA systems are required.

To address the 16-nm development need, SEMATECH has launched a program to develop 0.5-NA microfield exposure tools [14] with the goal of installing one of those tools at Lawrence Berkeley National Laboratory's Advanced Light Source synchrotron facility enabling the modified illumination discussed above at this even higher NA. Such illumination capabilities would allow this new tool to achieve resolution limits below 8 nm. Figure 11 shows a schematic of the 0.5-NA optical design which as with the 0.3-NA MET will be a centrally-obscured, two-element Schwarschild type optic. Also shown in Fig. 11 are the aerial-image modeling results for three different illumination conditions.

6. Acknowledgements

The authors are greatly indebted to Kevin Bradley, Rene Delano, Jeff Gamsby, Eric Gullikson, Bob Gunion, Gideon Jones, Ron Oort, Ron Tackaberry, and Farhad Salmassi for expert engineering, technical, and fabrication support. The authors are also grateful to

Shinji Tarutani of Fujifilm, and Jim Thackeray and Katherine Spear of Rohm and Haas for resist support. Finally the authors acknowledge the programmatic support from Frank Goodwin, Bryan Rice, and Stefan Wurm of SEMATECH. This work was supported by SEMATECH and carried out at Lawrence Berkeley National Laboratory's Advanced Light Source, which is supported by the Office of Science, Basic Energy Sciences, U.S. Department of Energy under Contract No. DE-AC02-05CH11231.

References

1. H. Meiling, et al., "First performance results of the ASML alpha demo tool," Proc. SPIE **6151**, 615108 (2006).

2. M. Miura, K. Murakami, K. Suzuki, Y. Kohama, Y. Ohkubo, T. Asami, "Nikon EUVL development progress summary," Proc. SPIE **6151**, 615105 (2006).

3. P. Naulleau, *et al.*, "Status of EUV micro-exposure capabilities at the ALS using the 0.3-NA MET optic," Proc. SPIE **5374**, 881-891 (2004).

4. A. Brunton, *et al*., "High-resolution EUV imaging tools for resist exposure and aerial image monitoring," Proc. SPIE **5751**, 78-89 (2005).

5. H. Oizumi, Y. Tanaka, I. Nishiyama, H. Kondo, K. Murakami, "Lithographic performance of high-numerical-aperture (NA=0.3) EUV small-field exposure tool (HINA)," Proc. SPIE **5751**, 102-109 (2005).

6. Prolith is a registered trademark of KLA-Tencor Corporation, 160 Rio Robles, San Jose, California 95134.

7. C. Koh, L. Ren, J. Georger, F. Goodwin, S. Wurm, B. Pierson, J. Park, T. Wallow, T. Younkin, and P. Naulleau, "Assessment of EUV resist readiness for 32nm hp manufacturing, and extendibility study of EUV ADT using state-of-the-art resist," Proc. SPIE **7271**, *to be published* (2009).

8. P. Naulleau, J. Cain, K. Dean, and K. Goldberg, "Lithographic Characterization of Low-Order Aberrations in a 0.3-NA EUV Microfield Exposure Tool," Proc. SPIE **6151**, 6151104 (2006).

9. J. Cain, P. Naulleau, E. Gullikson, C. Spanos, "Lithographic characterization of the flare in the Berkeley 0.3-numerical aperture extreme ultraviolet microfield optic," J. Vac. Sci. & Technol. B **24**, 1234-1237 (2006).

10. N. Beaudry, T. Milster, "Effects of mask roughness and condenser scattering in EUVL systems," Proc. SPIE. **3676**, 653-662 (1999).

11. P. Naulleau, "The relevance of mask-roughness-induced printed line-edge roughness in recent and future EUV lithography tests," Appl. Opt. **43**, 4025-4032 (2004).

12. P. Naulleau, D. Niakoula, G. Zhang, "System-level line-edge roughness limits in extreme ultraviolet lithography," J. Vac. Sci. & Technol. B **26**, 1289-1293 (2008).

13. P. Naulleau, "Correlation method for the measure of mask-induced line-edge roughness in extreme ultraviolet lithography," Appl. Opt., *to be published* (2009).

14. Michael Goldstein, Russ Hudyma, Patrick Naulleau, Stefan Wurm, "Extreme-ultraviolet Microexposure Tool at 0.5 NA for Sub-16 nm Lithography," Opt. Lett. **33**, 2995-2997 (2008).

List of Figures

Fig. 1. Modeling results of the limits of a tool with 0.25 NA and conventional disk illumination with coherence factor of 0.5. Optical parameters are set to 7% effective flare and 1 nm wavefront aberrations randomly distributed over Zernikes 5 through 37. Zernikes 1 through 4 are piston, x tilt, y tilt, and defocus, respectively.

Fig. 2. Aerial-image contrast as a function of half pitch for the SEMATECH Berkeley microfield exposure tool (BMET) with annular illumination illumination (0.35 < σ < 0.55). Flare and wavefront aberration values are taken from the literature [8,9].

Fig. 3. Aerial-image modeling results for four different resolution enhancing illumination settings in the BMET. In all cases vertical lines and spaces are modeled, however, the two 45°-rotated dipoles are capable of imaging Manhattan geometry (both horizontal and vertical lines).

Fig. 4. Direct comparison of printing and modeling results for radial gratings of varying half pitch using 45°-rotated dipole illumination with a pole radius of 0.15 and offset of 0.57. The orientation and pitch dependence of the imaging performance is clear and correlates well between modeling and experiment.

Fig. 5. Vertical lines and spaces printed in the BMET using the 45°-rotated dipole.

Fig. 6. Vertical lines and spaces printed in the BMET using the x-oriented dipole as depicted by the pupil-fill image in the figure.

Fig. 7. Scanning electron micrographs from the EUV reticle used on the BMET demonstrating that the mask itself also suffers from a limit of approximately 20 nm. Similar results have been found on masks from other suppliers.

Fig. 8. Cartoon showing the pseudo strong phase shift mask configuration with the centrally obscured BMET.

Fig. 9. BMET printing results using pseudo strong phase shift mask mode. On axis disk illumination with a coherence factor of 0.15 was used. The central obscuration of the BMET is 30% of the full pupil in radius.

Fig. 10. Aerial-image modeling results for the pseudo strong phase shift mask mode and assuming mask multilayer roughness. Also shown are the thresholded images showing the strong impact of mask effects on the LER.

Fig. 11. Schematic of the 0.5-NA optical design planned for the next generation BMET. Also shown are the aerial-image modeling results for three different illumination conditions.

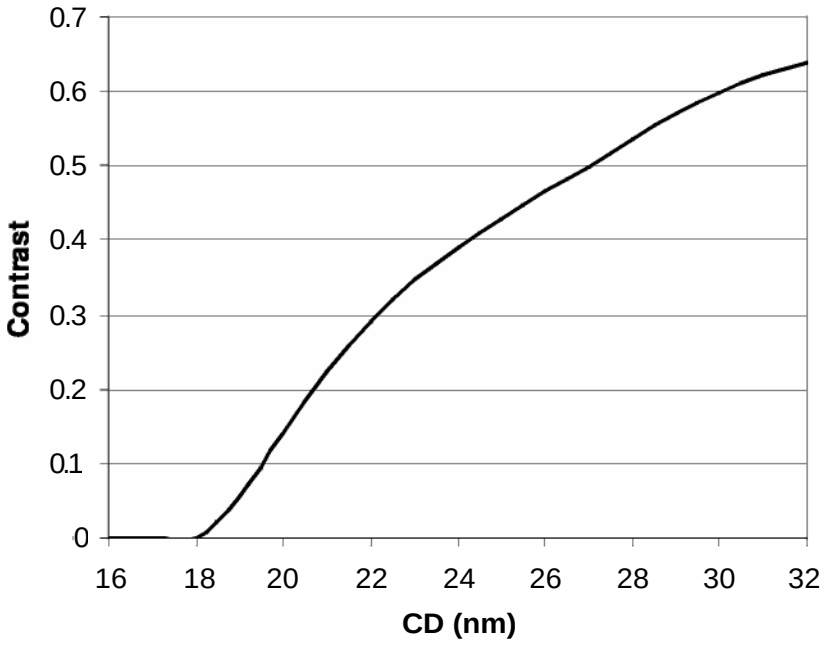

Fig. 1. Prolith-calculated aerial image contrast as a function of half pitch for a 0.25-NA EUV system under disk illumination (= 0.5) and assuming 7% effective flare and 1-nm rms wavefront aberration randomly distributed from Zernikes 5 through 37.

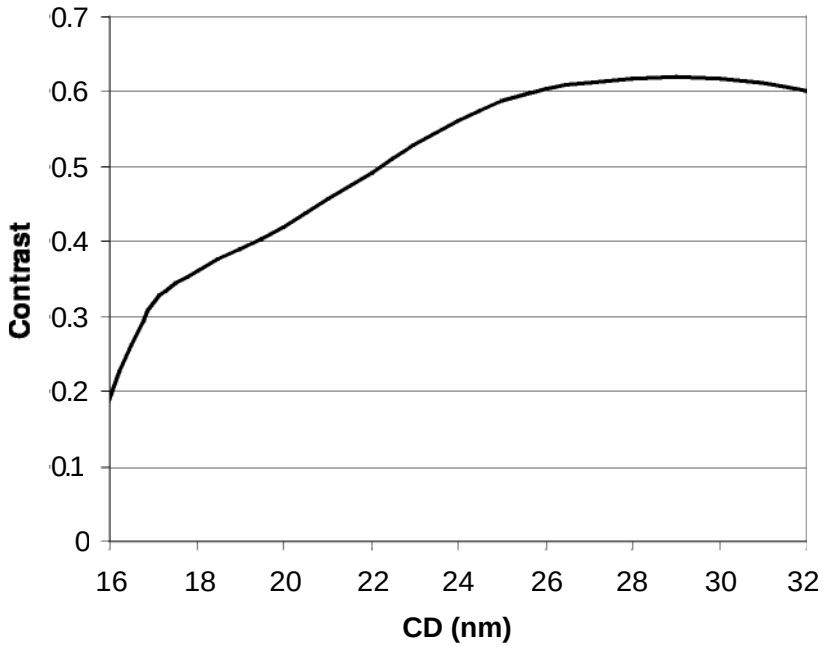

Fig. 2. Prolith-calculated aerial image contrast as a function of half pitch for the 0.3-NA BMET under annular illumination ($0.35 < \sigma < 0.55$) and assuming published flare and aberration values.

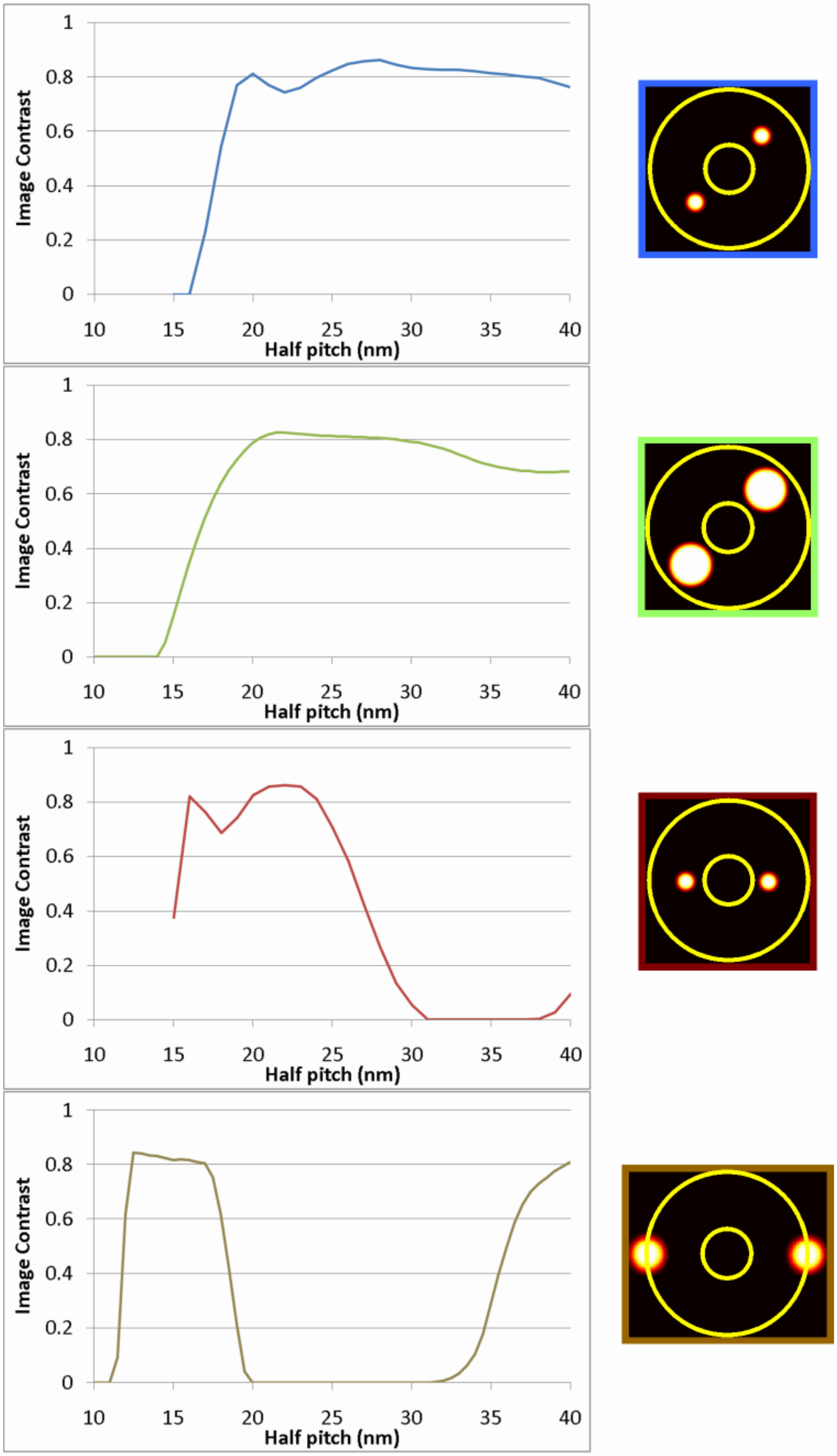
Image Contrast
Half pitch (nm)
0
0.2
0.4
0.6
0.8
1
10
15
20
25
30
35
40

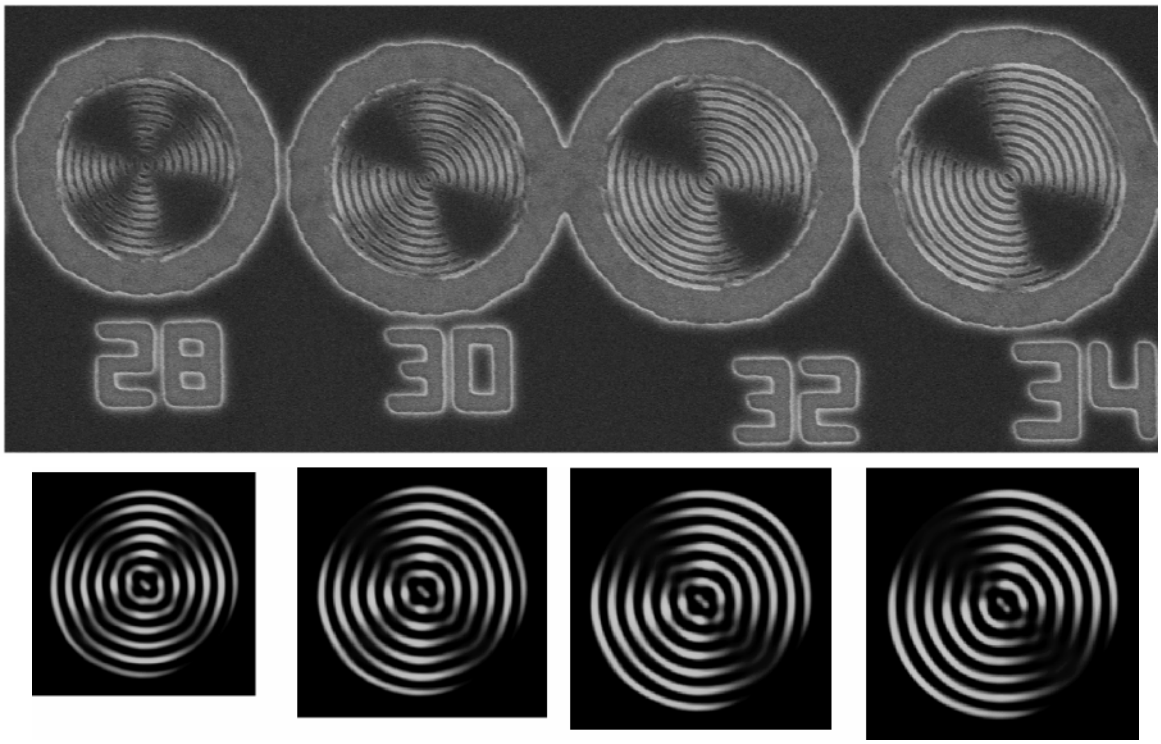

Fig. 4. Direct comparison of printing and modeling results for radial gratings of varying half pitch using 45°-rotated dipole illumination with a pole radius of 0.15 and offset of 0.57. The orientation and pitch dependence of the imaging performance is clear and correlates well between modeling and experiment.

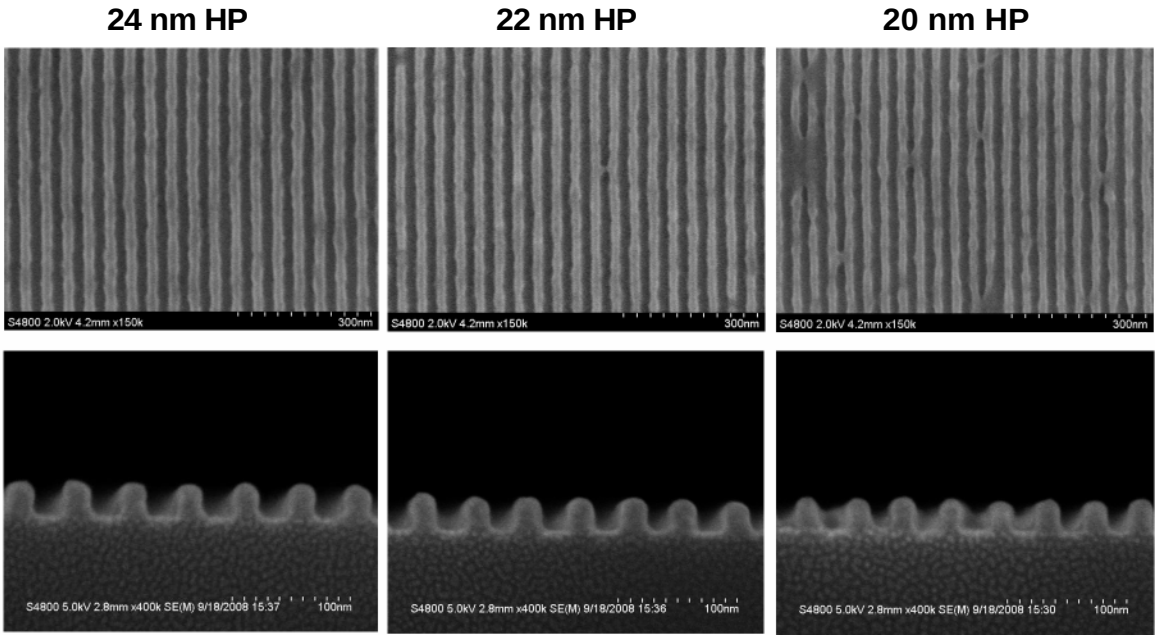

Fig. 5. Vertical lines and spaces printed in the BMET using the 45°-rotated dipole.

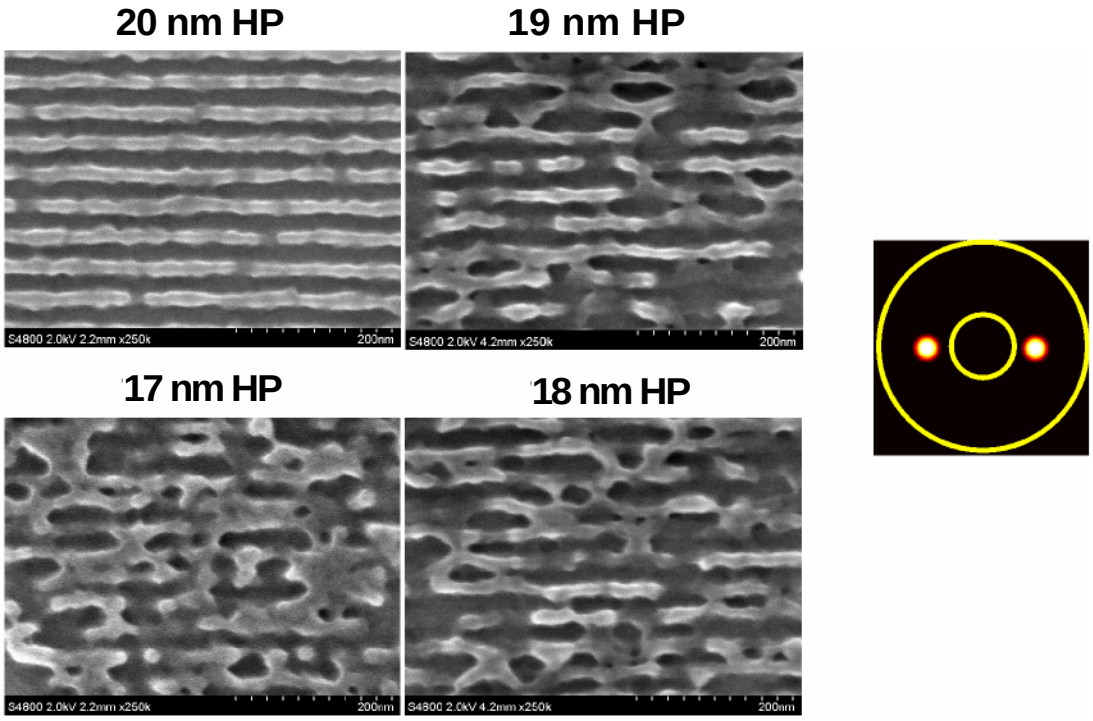

Fig. 6. Vertical lines and spaces printed in the BMET using the x-oriented dipole as depicted by the pupil-fill image in the figure.

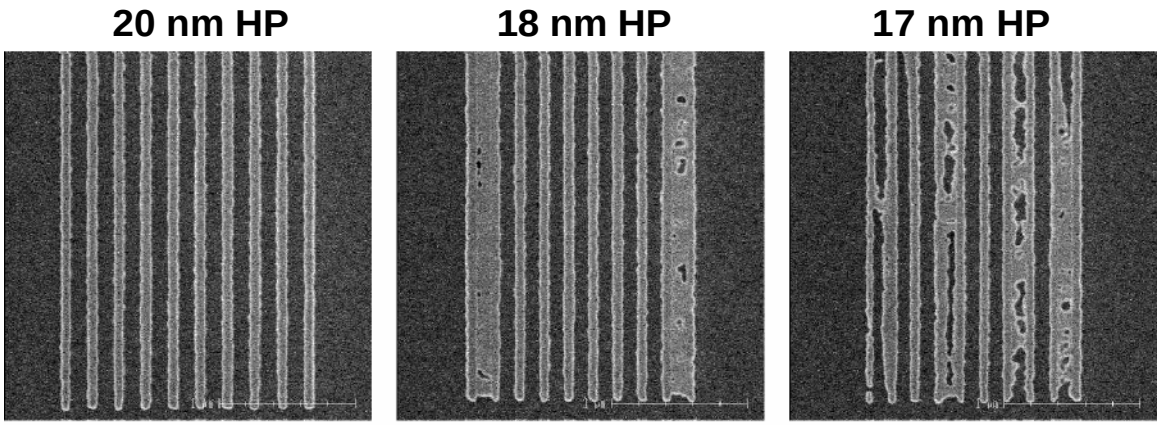

Fig. 7. Scanning electron micrographs from the EUV reticle used on the BMET demonstrating that the mask itself also suffers from a limit of approximately 20 nm. Similar results have been found on masks from other suppliers.

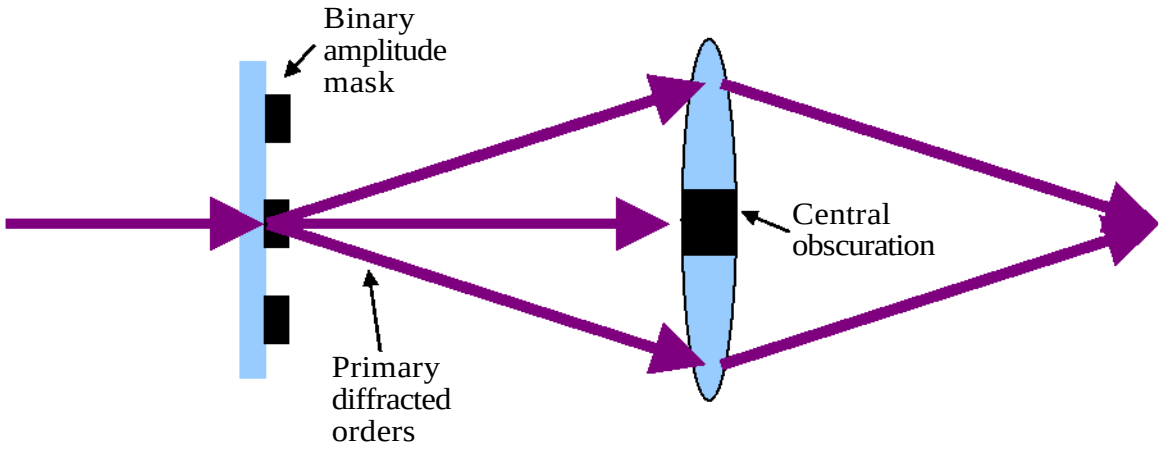

Fig. 8. Cartoon showing the pseudo strong phase shift mask configuration with the centrally obscured BMET.

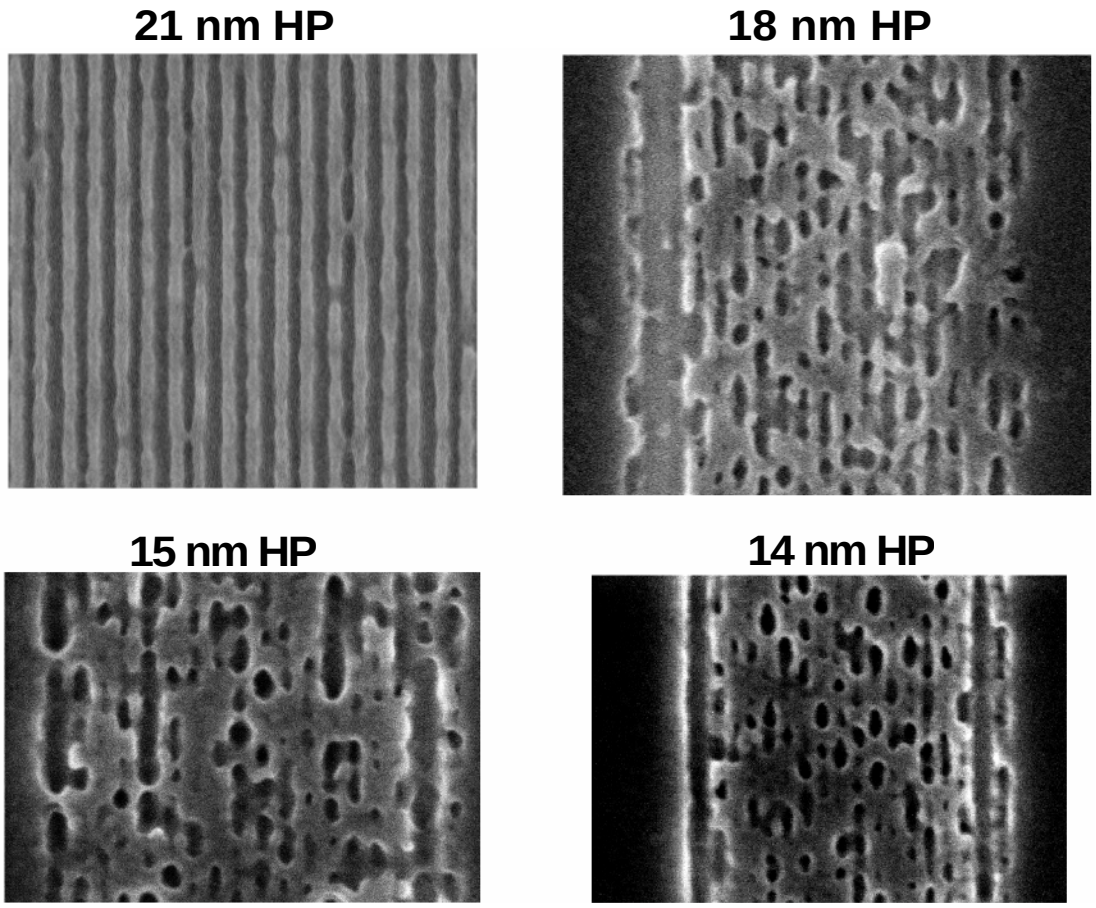

Fig. 9. BMET printing results using pseudo strong phase shift mask mode. On axis disk illumination with a coherence factor of 0.15 was used. The central obscuration of the BMET is 30% of the full pupil in radius.

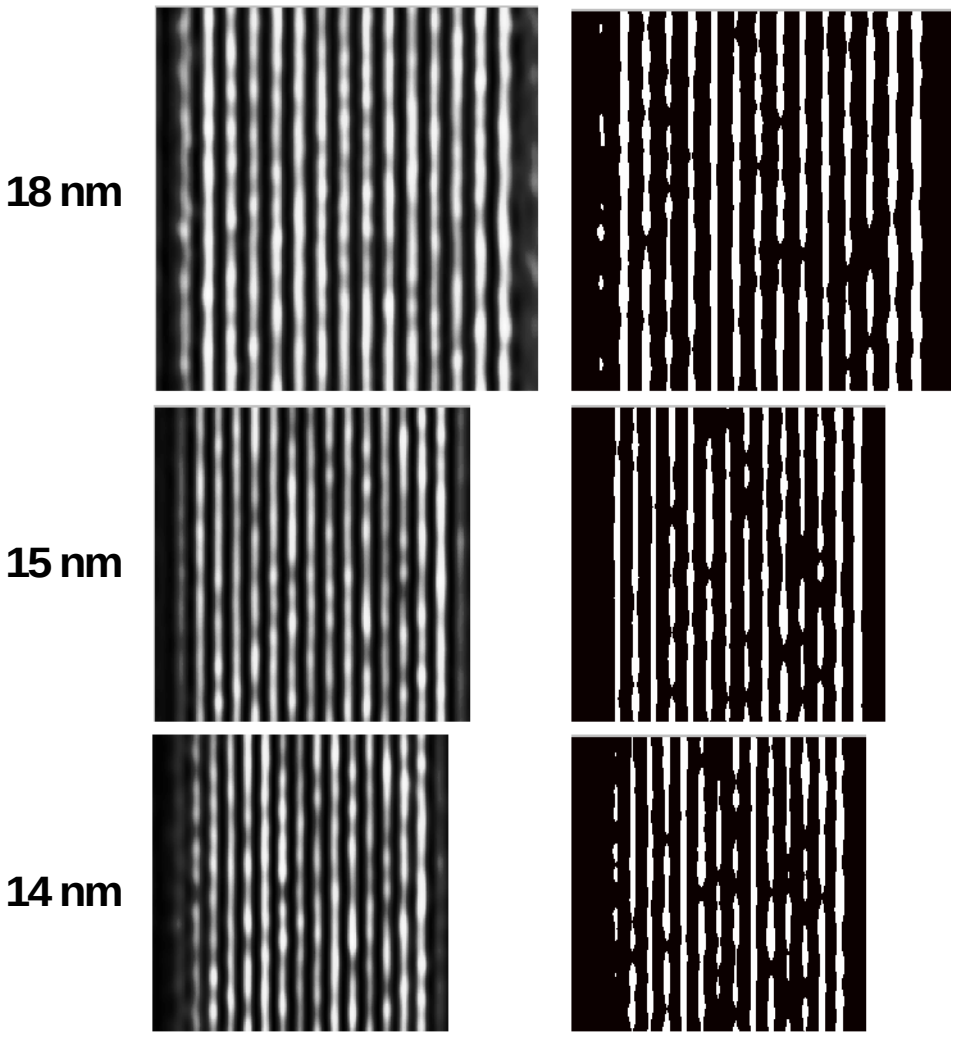

Fig. 10. Aerial-image modeling results for the pseudo strong phase shift mask mode and assuming mask multilayer roughness. Also shown are the thresholded images showing the strong impact of mask effects on the LER.

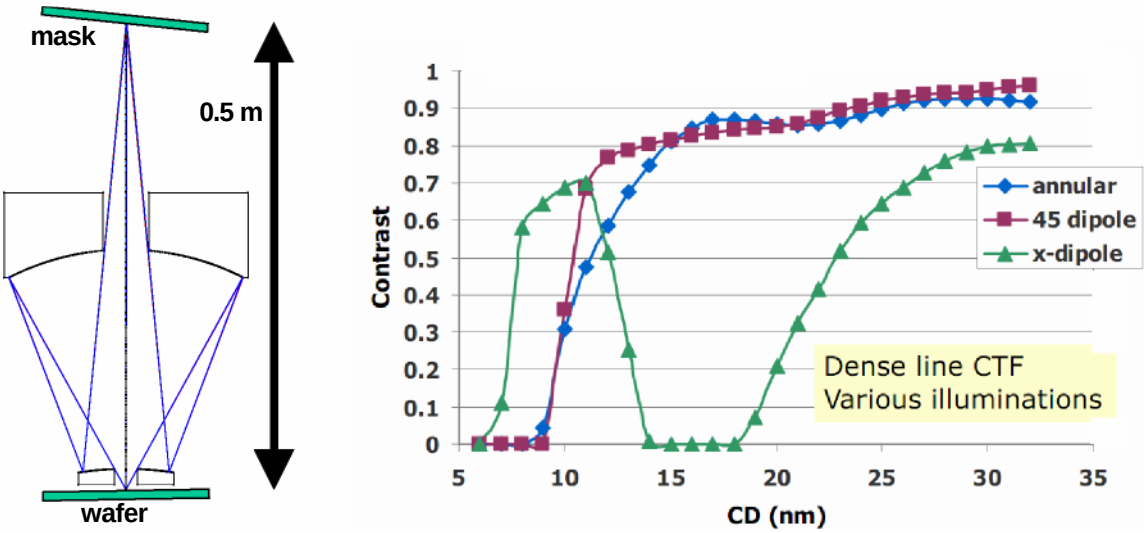

Fig. 11. Schematic of the 0.5-NA optical design planned for the next generation BMET. Also shown are the aerial-image modeling results for three different illumination conditions.